

# Theoretical uncertainties on quasielastic charged-current neutrino-nucleus cross sections

M. Valverde,<sup>1</sup> J. E. Amaro,<sup>1</sup> and J. Nieves<sup>1</sup>

<sup>1</sup>*Departamento de Física Moderna,  
Universidad de Granada, E-18071 Granada, Spain*

We estimate the theoretical uncertainties of the model developed in Phys. Rev. **C70** 055503 for inclusive quasielastic charged-current neutrino-nucleus reactions at intermediate energies. Besides we quantify the deviations of the predictions of this many body framework from those obtained within a simple Fermi gas model. A special attention has been paid to the ratio  $\sigma(\mu)/\sigma(e)$  of interest for experiments on atmospheric neutrinos. We show that uncertainties affecting this ratio are likely smaller than 5%

PACS numbers: 25.30.Pt, 13.15.+g, 24.10.Cn, 21.60.Jz

## I. INTRODUCTION

Recently an interest in neutrino scattering off nuclei has raised because of its implications in the experiments on neutrino oscillations based on large Cerenkov detectors. Atmospheric neutrino oscillations are dominantly due to  $\nu_\mu \rightarrow \nu_\tau$  flavor mixing, which has been already confirmed by the Super-Kamiokande experiments [1]. Future experiments aim at observing sub-leading effects on top of the dominant one [2], which are due to atmospheric  $\nu_e$  flavor oscillations. Observability of these effects depends strongly on the assumed experimental and theoretical systematic uncertainties. The most simple model regarding these effects supposes that these oscillations are controlled by neutrino masses (through their mass squared differences  $\Delta m^2$ ) and by a  $3 \times 3$  unitary mixing matrix similar to the CKM matrix in the quark sector, thus we are provided with  $3 + 9 + 1$  parameters not fully determined yet. To reduce the error size on these parameters requires an improvement in already existing neutrino detectors. These experiments use the nuclei in water as target for the incoming neutrinos, so a nuclear reaction model is needed for the data analyses. One of the main sources of systematical error in these experiments is precisely the cross sections for quasielastic (QE) neutrino scattering [3]. An accurate theoretical framework for the neutrino-nucleus dynamics, and a reliable estimate of the uncertainties affecting its predictions will definitely help to have a close control over the systematics affecting the oscillation parameters.

To describe Charged Current (CC) neutrino-nucleus reactions, we use here the Many Body Framework (MBF) developed in Ref. [4]<sup>1</sup>. Starting from a Local Fermi Gas (LFG) picture of the nucleus, which automatically accounts for Pauli blocking, several nuclear effects are taken into account in that scheme: *i*) a correct energy balance, using the experimental  $Q$ -values, is enforced, *ii*) Coulomb distortion of the charged leptons is implemented by using the so called “modified effective momentum approximation”, *iii*) medium polarization (RPA), including  $\Delta$ -hole degrees of freedom and explicit pion and rho exchanges in the vector-iso vector channel of the effective nucleon-nucleon force, and Short Range Correlation (SRC) effects are computed, and finally *iv*) the nucleon propagators are dressed in the nuclear medium, which amounts to work with a LFG of interacting nucleons and it also accounts for reaction mechanisms where the gauge boson,  $W^+$  or  $W^-$ , is absorbed by two nucleons. This model is a natural extension of previous studies on electron [6], photon [7] and pion [8, 9] dynamics in nuclei. Even though the scarce existing CC data involve very low nuclear excitation energies, for which specific details of the nuclear structure might play an important role, the model of Ref. [4] provides one of the best existing combined description of the inclusive muon capture in  $^{12}\text{C}$  and of the measurements of the  $^{12}\text{C}(\nu_\mu, \mu^-)X$  and  $^{12}\text{C}(\nu_e, e^-)X$  reactions near threshold. Inclusive muon capture from other nuclei is also successfully described by the model. Besides, above, let us say 80 or 100 MeV of energy transferred to the nucleus, this MBF leads also to excellent results for the  $(e, e')$  inclusive reaction in nuclei, not only in the QE region, but also when it is extended to the study of the  $\Delta$ -peak and the dip region (located between the QE and the  $\Delta$  peaks) [6]<sup>2</sup> and to the description of the absorption of real photons by nuclei [7].

In this work we pay a special attention to the source and size of the theoretical uncertainties affecting the predictions of Ref. [4]. Firstly, we have to locate the main inputs of the model and assign to each of them a reliable uncertainty.

<sup>1</sup> This model has been recently extended to the Neutral Current (NC) sector and to the study of nucleon knock-out reactions induced by neutrinos [5].

<sup>2</sup> Data in  $^{12}\text{C}$ ,  $^{40}\text{Ca}$  and  $^{208}\text{Pb}$  of differential cross sections for different electron kinematics and split into longitudinal and transverse response functions are successfully described.

For the experimentally determined parameters this obviously has to be determined by the experimental error, while for the model dependent parameters, we will assume theoretically founded sizes for their errors. Then we propagate the errors by means of a numerical simulation, that is: we consider the input parameters to be represented by uncorrelated Gaussian distributions, and by means of a Monte Carlo (MC) simulation, we find for any observable predicted by the model its derived probability distribution, which specific features will determine its associated theoretical uncertainty.

Besides, there exist some systematic errors associated to the validity of the hypothesis in which the scheme of Ref. [4] is based. Those are harder to estimate and we will discuss them at the end of this paper.

## II. SOURCES OF THEORETICAL ERRORS

The main inputs of the model of Ref. [4] are:

- *Lepton and hadron masses, electro weak coupling constants*, which we will assume to be errorless.
- *Neutrino-nucleon form factors*.

The neutrino-nucleon interaction is assumed to be of the  $V - A$  type. The vector form factors are related to the electromagnetic ones by means of the isospin symmetry, which we will consider exact. For the electromagnetic form factors we use the Galster parameterization [10],

$$F_1^N = \frac{G_E^N + \tau G_M^N}{1 + \tau}, \quad (1)$$

$$\mu_N F_2^N = \frac{G_M^N - G_E^N}{1 + \tau}, \quad (2)$$

$$\begin{aligned} G_E^p &= \frac{G_M^p}{\mu_p} = \frac{G_M^n}{\mu_n} = -(1 + \lambda_n \tau) \frac{G_E^n}{\mu_n \tau} \\ &= \left( \frac{1}{1 - q^2/M_D^2} \right)^2 \end{aligned} \quad (3)$$

with  $\tau = -q^2/4M^2$ ,  $M$  the nucleon mass,  $N$  standing for  $n$  (neutron) or  $p$  (proton) and  $\mu_N$  being the correspondent nucleon magnetic moment. The axial part is ruled by the axial form factor

$$G_A(q^2) = \frac{g_A}{(1 - q^2/M_A^2)^2} \quad (4)$$

The pseudoscalar  $G_P$  form factor is related to the axial one by means of the partially conserved axial current hypothesis (PCAC). The non-pole contribution to  $G_P$  at  $q^2 = 0$  is around 200 times smaller [11] than the pole contribution taken into account by means of PCAC. We will not explicitly consider this source of systematics, though we will assume an uncertainty for  $g_A$  larger than that generally used in the literature.

Thus, from these form factors we are left with four input parameters:  $M_D$ ,  $\lambda_n$ ,  $g_A$  and  $M_A$ , since we neglect any type of uncertainty in the nucleon magnetic moments. The Particle Data Group (PDG) compiles several determinations of  $g_A(0)/g_V(0)$ <sup>3</sup> from neutron beta decay studies, ranging most of them in the interval 1.25–1.27 [12], we will adopt a conservative point of view and we will take here  $1.26 \pm 0.01$ , though the average error quoted by the PDG is more than three times smaller. For the axial cutoff mass, we will assume  $1.05 \pm 0.14$  from the analysis of the  $\nu d \rightarrow \mu^- pp$  reaction carried out in Refs. [13, 14]. Finally we will take a 5% and 10% error on  $M_D$  and  $\lambda_n$ , respectively. Parameters are compiled in Table I.

- *The nuclear medium effective baryon–baryon interaction used in the computation of the RPA effects*. The effective nuclear interaction is included in the model starting from a particle-hole (ph) particle-hole interaction of the Landau-Migdal type

$$V = c_0 \{ f'_0(\rho) \vec{\tau}_1 \vec{\tau}_2 + g'_0(\rho) \vec{\sigma}_1 \vec{\sigma}_2 \vec{\tau}_1 \vec{\tau}_2 \}, \quad (5)$$

---

<sup>3</sup> We assume  $g_V(0) = 1$  according to the conserved vector current hypothesis.

since we are studying only CC induced reactions we have limited ourselves to the isovector channels. The  $\rho(r)$  dependence of  $f'_0$  is linearly parameterized as [15]

$$f'_0(\rho(r)) = \frac{\rho(r)}{\rho(0)} f'^{(in)}_0 + \left[1 - \frac{\rho(r)}{\rho(0)}\right] f'^{(ex)}_0 \quad (6)$$

Thus, we have from the  $\vec{\tau}\vec{\tau}$  channel three parameters:  $c_0$ ,  $f'^{(in)}_0$  and  $f'^{(ex)}_0$ . In the channel  $\vec{\sigma}\vec{\sigma}\vec{\tau}\vec{\tau}$  we use an interaction with explicit  $\pi$  (longitudinal) and  $\rho$  (transverse) exchanges and then we replace [8]

$$c_0 g'_0(\rho) \vec{\sigma}_1 \vec{\sigma}_2 \vec{\tau}_1 \vec{\tau}_2 \rightarrow \vec{\tau}_1 \vec{\tau}_2 \sum_{i,j=1}^3 \sigma_1^i \sigma_2^j V_{ij}^{\sigma\tau} \quad (7)$$

where

$$V_{ij}^{\sigma\tau} = (\hat{q}_i \hat{q}_j V_l(q) + (\delta_{ij} - \hat{q}_i \hat{q}_j) V_t(q)) \quad (8)$$

$\hat{q} = \vec{q}/|\vec{q}|$  is an unitary vector parallel to the transferred momentum and the strengths of the ph-ph interaction in the longitudinal and transverse channel are given by

$$\begin{aligned} V_t(q^0, \vec{q}) &= \frac{f^2}{m_\pi^2} \left\{ C_\rho \left( \frac{\Lambda_\rho^2 - m_\rho^2}{\Lambda_\rho^2 - q^2} \right)^2 \frac{\vec{q}^2}{q^2 - m_\rho^2} + g'_t(q) \right\}, \\ V_l(q^0, \vec{q}) &= \frac{f^2}{m_\pi^2} \left\{ \left( \frac{\Lambda_\pi^2 - m_\pi^2}{\Lambda_\pi^2 - q^2} \right)^2 \frac{\vec{q}^2}{q^2 - m_\pi^2} + g'_l(q) \right\} \end{aligned} \quad (9)$$

Besides,  $\Delta(1232)$  degrees of freedom are also taken into account in this channel. The ph- $\Delta h$  and  $\Delta h$ -ph effective interactions are obtained from the interaction of Eq. (7) by replacing  $\vec{\sigma} \rightarrow \vec{S}$ ,  $\vec{\tau} \rightarrow \vec{T}$ , where  $\vec{S}, \vec{T}$  are the spin, isospin  $N\Delta$  transition operators [8] and  $f \rightarrow f^* = 2.13 f$ , for any  $\Delta$  which replaces a nucleon. The SRC functions  $g'_l$  and  $g'_t$  have a smooth  $q$ -dependence [8], which we will not consider here, since we will explore only low and intermediate energies and momenta, and thus we will take  $g'_l(q) = g'_t(q) = g'$  [4, 6, 9]. Hence, we end up with six additional parameters:  $f$ ,  $f^*$ ,  $\Lambda_\pi$ ,  $C_\rho$ ,  $\Lambda_\rho$  and  $g'$ . We would like to point out that all these nine parameters, which are used to parameterize the medium effective baryon-baryon interaction, were adjusted long time ago [8, 15], and since then have been successfully used in several nuclear calculations at intermediate energies [6]–[9]. Here we have assumed uncorrelated Gaussian distributions with relative errors of 10%, for all these parameters (see Table I), except for the constant  $c_0$ , for which we have not considered any type of uncertainty, because it always appears multiplying the parameters  $f'^{(in)}_0$  and  $f'^{(ex)}_0$  that have already 10% error within our analysis.

- *The nucleon self-energy.*

The nucleon self-energy is used to dress the nucleon propagators in the medium. Its real part modifies the free nucleon dispersion relation, while the imaginary part takes into account two nucleon absorption reaction channels. The result of it is a quenching of the QE peak respect to the simple ph excitation calculation and a spreading of the strength, or widening of the peak. The integrated strength over energies is not much affected though. Most of the effect comes from the consideration of the real part of the nucleon selfenergy, as it was first pointed out in Ref. [5]<sup>4</sup>. The model of Ref. [4] uses the results of a semiphenomenological approach developed by Fernández de Córdoba and Oset in [16]. The nucleon selfenergy,  $\Sigma(p^0, \vec{p}; \rho)$ , calculated in this latter reference depends explicitly on the nucleon energy and momentum [16] and leads to nucleon spectral functions in good agreement with accurate microscopic approaches like the ones of Refs. [17]–[19]. Because in great part the model of Ref. [16] is not entirely microscopic, it is hard to identify its parameters. Here we have assumed a 10% relative error (Gaussian) for the nucleon selfenergy in the medium. Ten percent error is a reasonable choice, since it safely covers the existing differences between the results of Ref. [16] and the microscopic approaches of Refs. [17]–[19]. As discussed above, the change in the nucleon dispersion relation is more important than the inclusion of the small nucleon width in the medium, related to the quasielastic channels, which will account for

---

<sup>4</sup> See for instance solid (red) and dotted (magenta) lines in Fig.4 of that reference.

$W^\pm$  absorption by two nucleons. Neglecting completely the imaginary part of the nucleon selfenergy leads to a considerable reduction in computation time and given the quality of this approximation, it has been used in all MC simulations performed to estimate the theoretical uncertainties of the results of Ref. [4].

- *Proton and Neutron matter densities.*

Charge densities are taken from [21] and proton densities are deduced from them. On the other hand, neutron densities are taken approximately equal (but normalized to the number of neutrons) to the proton ones, though small changes are considered, inspired by Hartree-Fock calculations with the density-matrix expansion [22] and corroborated by pionic atom data [23]. In this work we will present results for oxygen, carbon and argon, for the first two we use a modified harmonic oscillator distribution MHO (parameters can be found in Table I of Ref. [4]), while for argon we use a two-parameter Fermi distribution (parameters can be found in Table I of Ref. [5]). We take a 5% relative error (Gaussian uncorrelated) for all parameters, which is about one order of magnitude larger than the quoted errors for charge density parameters, but that safely covers uncertainties related to the neutron distributions and to the procedure of taking out the finite size of the proton and neutron particles.

### III. RESULTS AND CONCLUDING REMARKS

By means of a Monte Carlo simulation, we generate a total of 2000 sets of input parameters<sup>5</sup> from an uncorrelated multidimensional Gaussian distribution, with central values and standard deviations compiled in Table I. For each of the sample sets, we compute the different observables discussed in this work, and thus we obtain the distributions of all of them. Theoretical errors and uncertainty bands on the derived quantities are always obtained by discarding the highest and lowest 16% of the sample values, to leave a 68% Confidence Level (CL).

In Figs. 1 and 2, we present electron and muon neutrino inclusive QE integrated cross sections from carbon, oxygen and argon. Several comments are in order,

- As mentioned above, the imaginary part of the nucleon selfenergy has been neglected when performing the MC simulation. Let us look at Fig. 1, as can be appreciated there, the differences between the central line<sup>6</sup> of the 68% CL band and the full model prediction, which includes the effects of the imaginary part of  $\Sigma$ , are almost negligible and significantly smaller than the size of the 68% CL errors. This corroborates the findings of Ref. [5], and though, we will make graphically such a comparison in most of the plots that will be presented in what follows, we will not make any further comment about it.
- Nuclear effects beyond implementing Pauli's exclusion principle and enforcing the correct energy balance are sizeable and much larger than the uncertainties on the predictions deduced from the MBF presented in Ref. [4].
- In oxygen, we estimate separately the uncertainties (error bars<sup>7</sup> in the middle plots of Fig. 1) due to the imprecise knowledge of the nucleon densities and of the parameters entering in the model used in Ref. [4] to compute nuclear effects (RPA and nucleon self-energy). The value of the relative uncertainty due to nuclear effects decrease with energy, while relative errors induced by the neutrino-nucleon form factors increase with energy, and at the higher end, they could be comparable to those affecting the evaluation of the nuclear effects.
- Uncertainties on the integrated cross sections are of the order of 10–15%, which turn out to be similar to those assumed for the input parameters (Table I). Hence, predictions of Ref. [4] seems stable. On the other hand, this also shows that there exist no fine tuning parameters in the MBF developed in [4].
- As can be appreciated in Fig. 2 for two particular cases, theoretical uncertainties on the cross section can be, in a good approximation, modeled by a Gaussian distribution.

Conclusions are similar for differential cross sections. As an example, in Fig. 3 we show the electron neutrino inclusive QE double differential cross section, at a fixed lepton momentum transfer, in oxygen as a function of the lepton energy transfer.

---

<sup>5</sup> We have checked that the errors quoted in the following are already stable when 1500 event simulations are performed.

<sup>6</sup> It has been obtained with the central values of the parameters quoted in Table I and neglecting the imaginary part of the nucleon selfenergy.

<sup>7</sup> Hence, these error bars do not take into account the uncertainties of the neutrino-nucleon form factors.

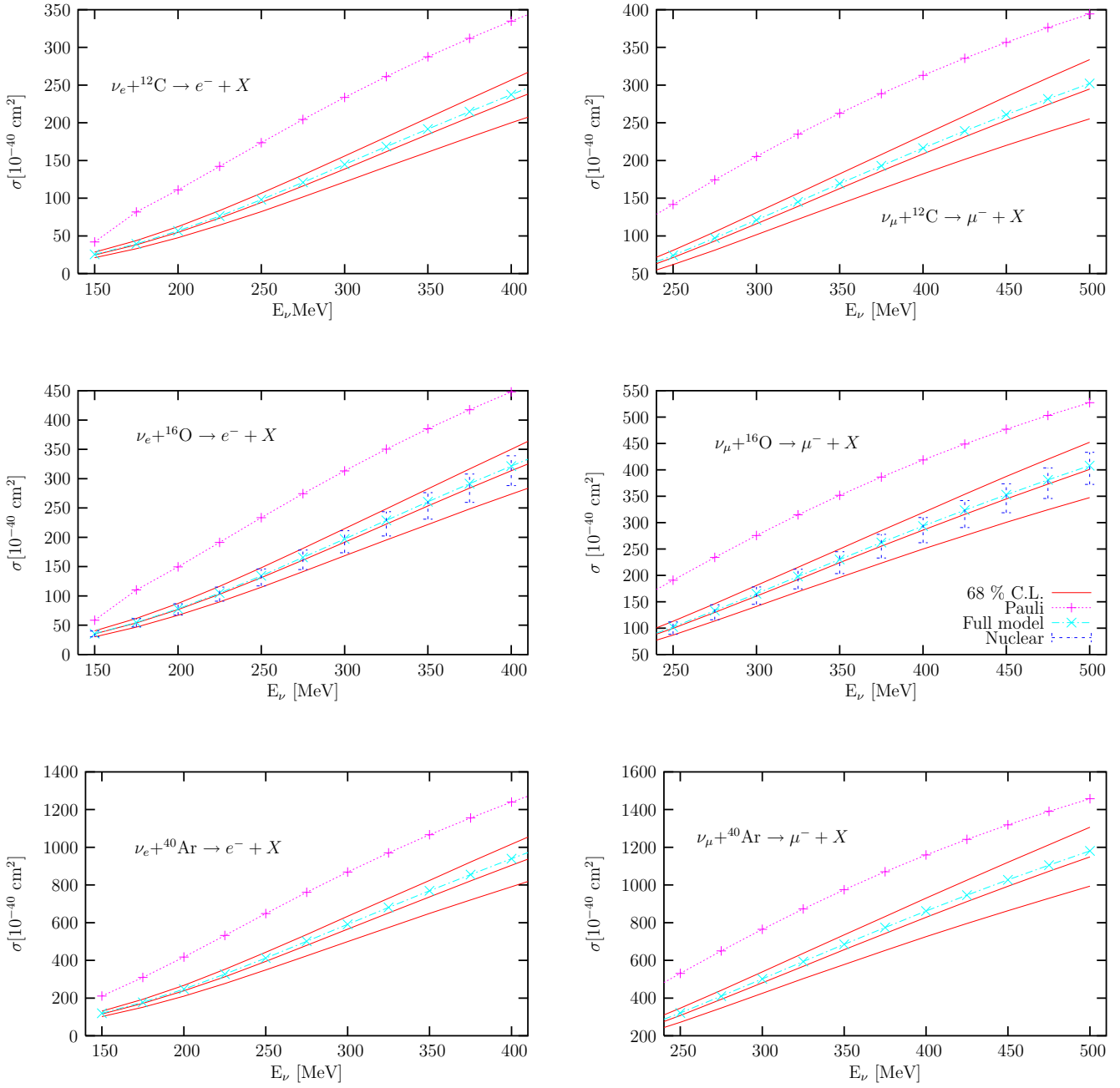


FIG. 1: (Color online) Electron and muon neutrino inclusive QE integrated cross sections from carbon, oxygen and argon, as a function of the neutrino energy. In all cases non-relativistic nucleon kinematics has been employed. Results denoted as “Full model” are obtained from the full model developed in Ref. [4], while those denoted as “Pauli” have been obtained without including RPA, Coulomb and nucleon selfenergy effects. We also give the 68% CL band (red or solid lines). For oxygen, the error bars (denoted as “Nuclear”) account for the uncertainties due to the imprecise knowledge of the nucleon densities and of the parameters entering in the model used (Ref. [4]) to compute nuclear effects (RPA and nucleon self-energy).

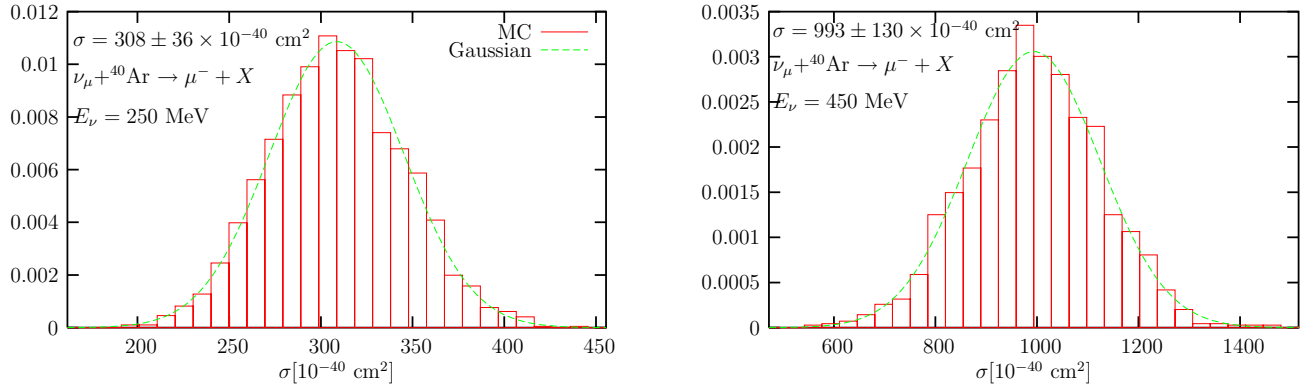


FIG. 2: (Color online) MC uncertainty distributions for muon neutrino inclusive QE integrated cross section from argon, at 250 (left) and 450 (right) MeV incoming neutrino energies. The dashed lines stand for Gaussian distributions with central values and variances indicated in each panel.

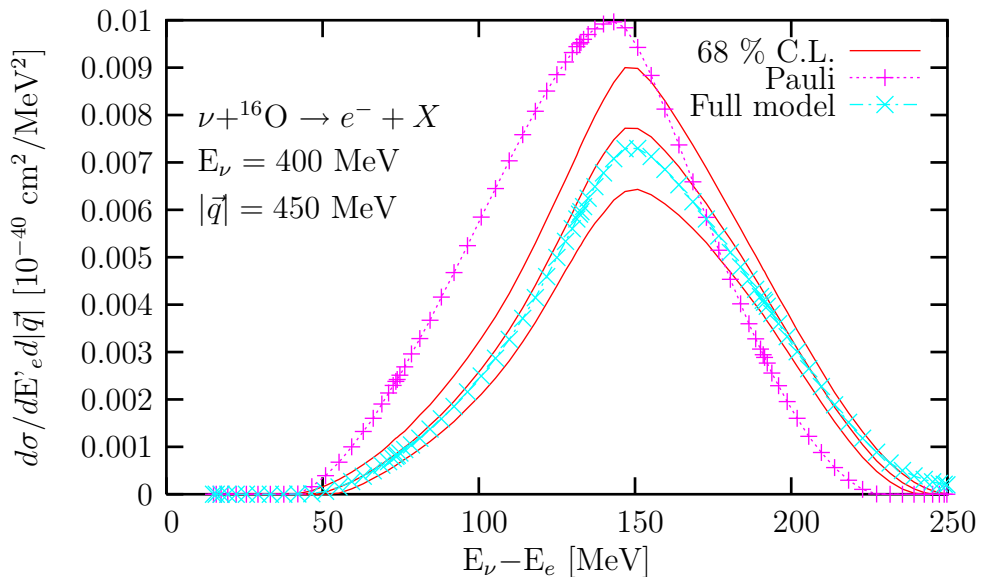


FIG. 3: (Color online) Electron neutrino inclusive QE differential cross section, at a fixed lepton momentum transfer of 450 MeV, in oxygen as a function of the lepton energy transfer. The incoming neutrino energy is 400 MeV and non-relativistic nucleon kinematics has been employed. Results denoted as “Full model” are obtained from the full model developed in Ref. [4], while those denoted as “Pauli” have been obtained without including RPA, Coulomb and nucleon selfenergy effects. We also give the 68% CL band (red or solid lines).

Theoretical errors cancel partially out in the ratio  $\sigma(\mu)/\sigma(e) \equiv \sigma(\nu_\mu + {}^A Z \rightarrow \mu^- + X)/\sigma(\nu_e + {}^A Z \rightarrow e^- + X)$ , as can be appreciated in Fig. 4. Theoretical uncertainties on this ratio turn out to be smaller than 1%. On the other

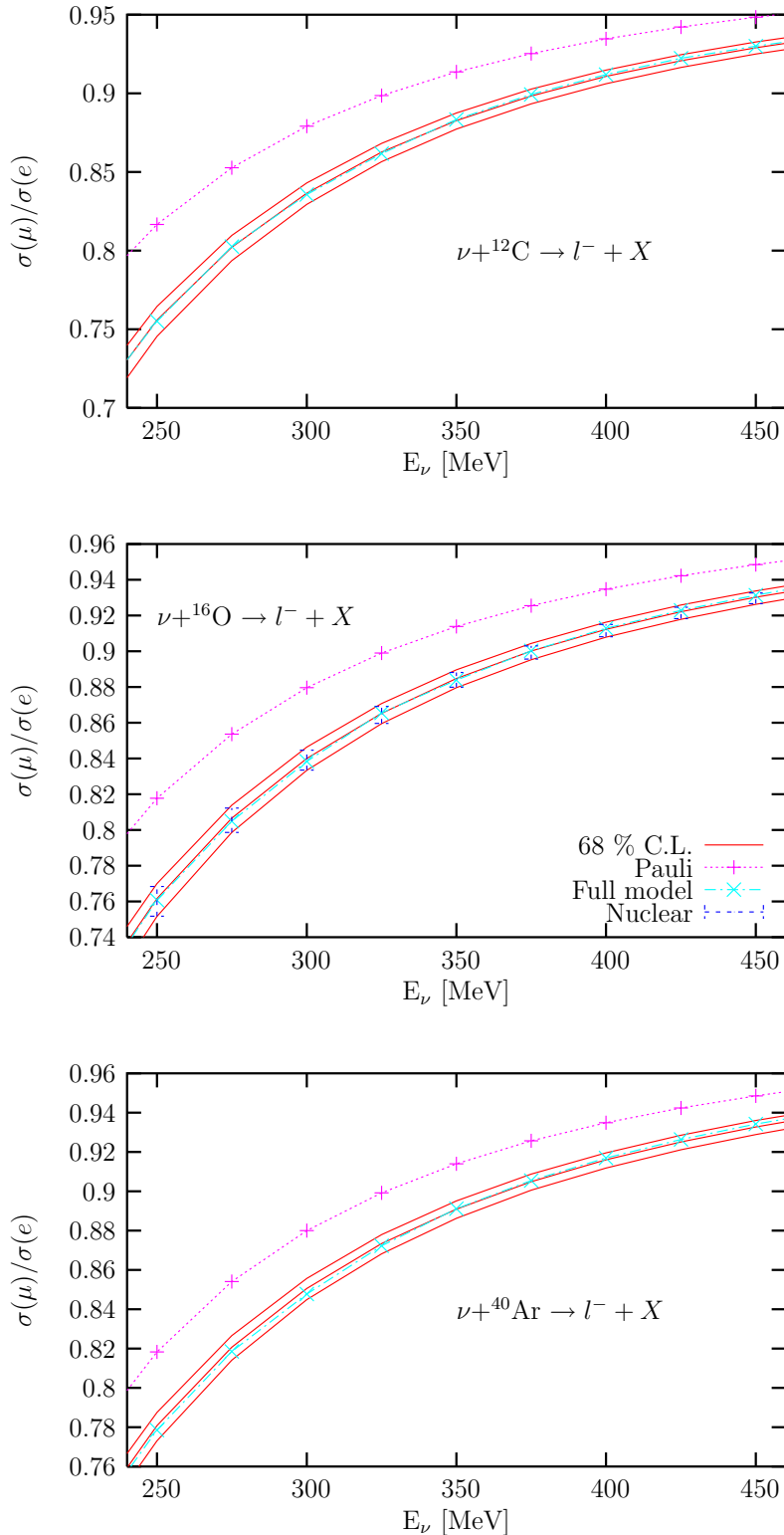


FIG. 4: (Color online) Ratio of inclusive QE cross sections  $\sigma(\mu)/\sigma(e)$  for carbon, oxygen and argon, as a function of the incoming neutrino energy. In all cases non-relativistic nucleon kinematics has been employed. Besides, the 68% CL band (red or solid lines), we also give results (crosses) from the full model developed in Ref. [4], and from the latter model without including RPA, Coulomb and nucleon selfenergy effects (line denoted as “Pauli”). For oxygen, the error bars have the same meaning as in Figs. 1 and 3.

Form Factors		Nucleon Interaction
$M_D = 0.843 \pm 0.042$ GeV	$f_0^{(in)} = 0.33 \pm 0.03$	
$\lambda_n = 5.6 \pm 0.6$	$f_0^{(tex)} = 0.45 \pm 0.05$	
$M_A = 1.05 \pm 0.14$ GeV	$f = 1.00 \pm 0.10$	
$g_A = 1.26 \pm 0.01$	$f^* = 2.13 \pm 0.21$	
	$\Lambda_\pi = 1200 \pm 120$ MeV	
	$C_\rho = 2.0 \pm 0.2$	
	$\Lambda_\rho = 2500 \pm 250$ MeV	
	$g' = 0.63 \pm 0.06$	

TABLE I: Central values and errors of the model input parameters, besides we have also included 10% uncertainties (relative) in both the real part of the nucleon selfenergy and densities (see text for details).

hand, predictions for this ratio obtained from a simple Lindhard function<sup>8</sup> incorporating a correct energy balance in the reaction (lines denoted as “Pauli” in the plots) differ from the results obtained from the model of Ref. [5] only at the level of 5%, in sharp contrast with the situation found for each of the the individual cross sections  $\sigma(\nu_\mu + {}^A Z \rightarrow \mu^- + X)$  and  $\sigma(\nu_e + {}^A Z \rightarrow e^- + X)$  (see Fig. 1). Finally, here we also find that the theoretical uncertainties on the ratio  $\sigma(\mu)/\sigma(e)$  can be, in a good approximation, modeled by a Gaussian distribution, as can be seen in Fig. 5.

For antineutrino induced reactions we find a totally parallel scenario to that discussed so far for neutrino-induced ones.

To finish this work, we would like to discuss some other systematic errors associated to the validity of the hypothesis in which the scheme of Ref. [4] is based, and not considered so far. In first place, up to this point a non-relativistic nucleon kinematics has been employed. This is because the RPA and nucleon selfenergy models used in Ref. [4] are based in a non-relativistic effective baryon–baryon interaction in the nuclear medium. The use of relativistic kinematics for the nucleons leads to moderate reductions of both neutrino and antineutrino cross sections, ranging these reductions in the interval 4–9%, at the intermediate energies considered in this work. Such corrections do not depend significantly on the considered nucleus [4]. In the ratio  $\sigma(\mu)/\sigma(e)$ , relativistic nucleon kinematics effects are quite small, being always smaller than 1% in the whole neutrino energy interval studied in this work, as can be seen in Fig. 6.

Second, one might think that a LFG description of the nucleus is poor, and that a proper finite nuclei treatment is necessary. For inclusive processes and nuclear excitation energies of around 100 MeV or higher, the findings of Refs. [6], [7] and [9] clearly contradict this conclusion. The reason is that in these circumstances one should sum up over several nuclear configurations, both in the discrete and in the continuum, and this inclusive sum is almost not sensitive to the details of the nuclear wave function<sup>9</sup>, in sharp contrast to what happens in the case of exclusive processes where the final nucleus is left in a determined nuclear level. On the other hand, the LFG description of the nucleus allows for an accurate treatment of the dynamics of the elementary processes (interaction of gauge bosons with nucleons, nucleon resonances, and mesons, interaction between nucleons or between mesons and nucleons, etc.) which occur inside the nuclear medium. Within a finite nuclei scenario, such a treatment becomes hard to implement, and often the dynamics is simplified in order to deal with more elaborated nuclear wave functions. This simplification of the dynamics cannot lead to a good description of nuclear inclusive electroweak processes at the intermediate energies of interest for future neutrino experiments.

<sup>8</sup> It is to say from a non-interacting local Fermi gas model of non-relativistic nucleons.

<sup>9</sup> The results of Ref. [4] for the inclusive muon capture in nuclei through the whole periodic table, where the capture widths vary from about  $4 \times 10^4$  s<sup>-1</sup> in  ${}^{12}\text{C}$  to  $1300 \times 10^4$  s<sup>-1</sup> in  ${}^{208}\text{Pb}$ , and of the LSND measurements of the  ${}^{12}\text{C}(\nu_\mu, \mu^-)X$  and  ${}^{12}\text{C}(\nu_e, e^-)X$  reactions near threshold indicate that the predictions of our scheme, for totally integrated inclusive observables, could even be extended to much smaller, of the order of 10 or 20 MeV, nuclear excitation energies. In this respect, the works of Refs. [24] and [25] for inclusive muon capture and radiative pion capture in nuclei, respectively, turn out to be quite enlightening. In those works, continuum shell model results are compared to those obtained from a LFG model for several nuclei from  ${}^{12}\text{C}$  to  ${}^{208}\text{Pb}$ . The differential decay width shapes predicted for the two set of models are substantially different. Shell model distributions present discrete contributions and in the continuum appear sharp scattering resonances. Despite the fact that those distinctive features do not appear in the LFG differential decay widths, the totally integrated widths (inclusive observable) obtained from both descriptions of the process do not differ in more than 5 or 10%. The typical nuclear excitation energies in muon and radiative pion capture in nuclei are small, of the order of 20 MeV, and thus one expects that at higher excitation energies, where one should sum up over a larger number of nuclear final states, the LFG predictions for inclusive observables would become even more reliable.

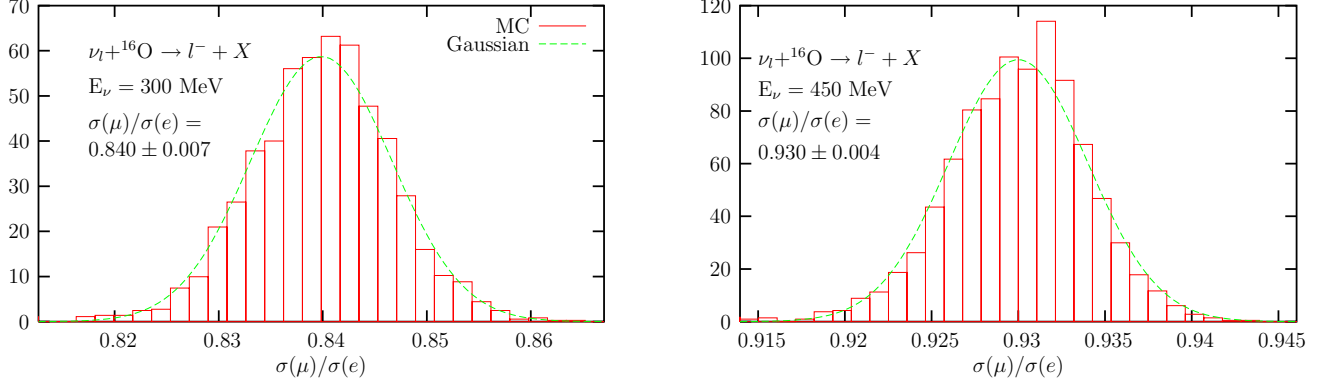


FIG. 5: (Color online) MC uncertainty distributions for the ratio of inclusive QE cross sections  $\sigma(\mu)/\sigma(e)$  from oxygen, at 300 (left) and 450 (right) MeV incoming neutrino energies. The dashed lines stand for Gaussian distributions with central values and variances indicated in each panel.

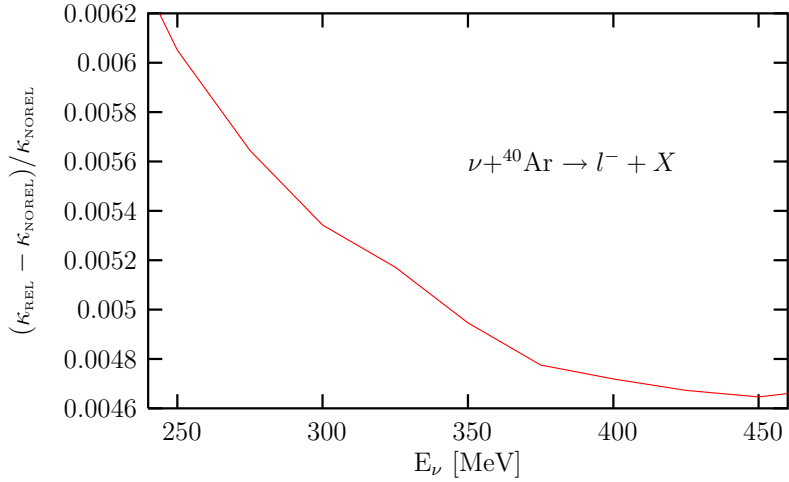


FIG. 6: (Color online) Relative corrections to the ratio  $\sigma(\mu)/\sigma(e)$ , in argon, due to the use of relativistic nucleon kinematics. We denote by  $\kappa_{\text{REL}}$  ( $\kappa_{\text{NOREL}}$ ) the ratio  $\sigma(\mu)/\sigma(e)$  deduced from a non-interacting local Fermi gas model of relativistic (non-relativistic) nucleons improved by the use of the experimental  $Q$ -values (see Ref. [4] for some more details). Thus,  $\kappa_{\text{NOREL}}$  would be given by the line denoted by ‘‘Pauli’’ in the argon panels of Fig. 4.

For all of this, it is sound to assume that the model of Ref. [4] provides QE neutrino–nucleus cross sections at intermediate energies with relative errors of about 10–15%, while uncertainties affecting the ratio  $\sigma(\mu)/\sigma(e)$  would be certainly smaller, likely not larger than about 5%, and mostly coming from deficiencies of the LFG picture of the nucleus assumed in Ref. [4].

### Acknowledgments

J.N. warmly thanks to M. J. Vicente-Vacas for various stimulating discussions and communications. This work was supported by DGI and FEDER funds, contract BFM2005-00810, by the EU Integrated Infrastructure Initiative Hadron Physics Project contract RII3-CT-2004-506078 and by the Junta de Andalucía.

---

[1] Super-Kamiokande Collaboration (Y. Fukuda *et al.*), Phys. Rev. Lett. **81** (1998) 1562; Y. Fukuda *et al.*, Phys. Lett. B **433**, 9 (1998).

[2] Proceedings of the RCCN International Workshop On Sub-dominant Oscillation Effects in Atmospheric Neutrino Experiments Kashiwa, 2004, Eds. T. Kajita and K. Okumura, Universal Academy Press, Inc. Tokyo, Japan

[3] T. Kajita and Y. Totsuka, Rev. Mod. Phys. **73**, 85 (2001).

[4] J. Nieves, J. E. Amaro, and M. Valverde, Phys. Rev. C **70**, 055503 (2004) [Erratum-*ibid.* C **72**, 019902 (2005)].

[5] J. Nieves, M. Valverde and M.J. Vicente-Vacas, Phys. Rev. C **73** 025504 (2006).

[6] A. Gil, J. Nieves and E. Oset, Nucl. Phys. **A627** (1997) 543; *ibidem*, Nucl. Phys. **A627** (1997) 599.

[7] R.C. Carrasco and E. Oset, Nucl. Phys. **A536** (1992) 445.

[8] E. Oset, H. Toki and W. Weise, Phys. Rep. **83** (1982) 281.

[9] L.L. Salcedo, E. Oset, M.J. Vicente-Vacas and C. García Recio, Nucl. Phys. **A484** (1988) 557; J. Nieves, E. Oset, C. García-Recio, Nucl. Phys. **A554** (1993) 509; *ibidem* Nucl. Phys. **A554** (1993) 554; J. Nieves and E. Oset, Phys. Rev. C **47** (1993) 1478; E. Oset, P. Fernández de Córdoba, J. Nieves, A. Ramos and L.L. Salcedo, Prog. Theor. Phys. Suppl. **117** (1994) 461; C. Albertus, J.E. Amaro and J. Nieves, Phys. Rev. Lett. **89** (2002) 032501; *ibidem* Phys. Rev. C **67** (2003) 034604.

[10] S. Galster, H. Klein, J. Moritz, K. H. Schmidt, D. Wegener, and J. Bleckwenn, Nucl. Phys. **B32** 221 (1971).

[11] V. Bernard, L. Elouardhiri, U.-G. Meissner, J. Phys. **G28** (2002) R1; D. Barquilla-Cano, A.J. Buchmann, E. Hernández, Nucl. Phys. **A714** (2003) 611.

[12] S. Eidelman, *et al.*, Phys. Lett. **B592** (2004) 1.

[13] N. J. Baker *et al.*, Phys. Rev **D23** (1981) 2499.

[14] T. Kitagaki *et al.*, Phys. Rev **D42** (1990) 1331.

[15] J. Speth, E. Werner, and W. Wild, Phys. Rep. **33** 127 (1977); J. Speth, V. Klemt, J. Wambach, and G. E. Brown Nucl. Phys. **A343** 382 (1980).

[16] P. Fernández de Córdoba and E. Oset, Phys. Rev. **C46** (1992) 1697.

[17] S. Fantoni, B.L. Friman, and V.R. Pandharipande, Nucl. Phys. **A399** (1983) 51; S. Fantoni and V.R. Pandharipande, Nucl. Phys. **A427** (1984) 473.

[18] C. Mahaux, P.F. Bortignon, R.A. Broglia, and C.H. Dasso, Phys. Rep. **120** (1985) 1.

[19] A. Ramos, A. Polls, and W. H. Dickhoff, Nucl. Phys. **A503** (1989) 1

[20] H. Müther, G. Knehr and A. Polls, Phys. Rev. **C52** (1995) 2955.

[21] C. W. de Jager, H. de Vries, and C. de Vries, At. Data and Nucl. Data Tables **14** 479 (1974); **36** 495 (1987).

[22] J.W. Negele and D. Vautherin, Phys. Rev. **C11** (1975) 1031 and references therein.

[23] C. García-Recio, J. Nieves and E. Oset, Nucl. Phys. **A547** (1992) 473

[24] J.E. Amaro, C. Maieron, J. Nieves and M. Valverde, Eur. Phys. Jour. **A24** (2005) 343 [Erratum-*ibid.* **A26**, 307 (2005)].

[25] J.E. Amaro, A.M. Lallena and J. Nieves, Nucl. Phys. **A623** (1997) 529.